Brain Network Analysis From High-Resolution EEG Recordings by the Application of Theoretical Graph Indexes

F. De Vico Fallani, L. Astolfi, F. Cincotti, D. Mattia, A. Tocci, S. Salinari, M. G. Marciani, H. Witte, A. Colosimo, and F. Babiloni

***Abstract*—The extraction of the salient characteristics from brain connectivity patterns is an open challenging topic since often the estimated cerebral networks have a relative large size and complex structure. Since a graph is a mathematical representation of a network, which is essentially reduced to nodes and connections between them, the use of a theoretical graph approach would extract significant information from the functional brain networks estimated through different neuroimaging techniques. The present work intends to support the development of the "brain network analysis:" a mathematical tool consisting in a body of indexes based on the graph theory able to improve the comprehension of the complex interactions within the brain. In the present work, we applied for demonstrative purpose some graph indexes to the time-varying networks estimated from a set of high-resolution EEG data in a group of healthy subjects during the performance of a motor task. The comparison with a random benchmark allowed extracting the significant properties of the estimated networks in the representative Alpha (7–12 Hz) band. Altogether, our findings aim at proving how the brain network analysis could reveal important information about the time-frequency dynamics of the functional cortical networks.**

***Index Terms*—High-resolution electroencephalography (EEG), functional networks, graph theory.**

Manuscript received December 28, 2008; revised May 27, 2008; accepted June 07, 2008. First published September 19, 2008; current version published November 05, 2008. This work was performed with the support of the COST EU project NEUROMATH (BM 0601) of the Minister for Foreign Affairs, Division for the Scientific and Technologic Development in the framework of a bilateral project between Italy and China (Tsinghua University) of the "Fondazione Banca Nazionale Comunicazioni." This paper only reflects the authors' views and funding agencies are not liable for any use that may be made of the information contained herein.

F. De Vico Fallani is with the IRCCS Fondazione Santa Lucia, 00179 Rome, Italy, and also with the CISB, University of Rome "Sapienza," 00186 Rome, Italy (e-mail: fabrizio.devicofallani@uniroma1.it).

L. Astolfi is with the IRCCS Fondazione Santa Lucia, 00179 Rome, Italy, and also with the DIS, University of Rome "Sapienza," 00185 Rome, Italy (e-mail: laura.astolfi@uniroma1.it).

F. Cincotti, D. Mattia, and A. Tocci are with the IRCCS Fondazione Santa Lucia, 00179 Rome, Italy (e-mail: f.cincotti@hsantalucia.it; d.mattia@hsantalucia.it).

S. Salinari is with the DIS, University of Rome "Sapienza," 00185 Rome, Italy (e-mail: salinari@dis.uniroma1.it).

M.G. Marciani is with the Neuroscience Department, University of Rome "Tor Vergata," 00133 Rome, Italy (e-mail: marciani@dis.uniroma2.it).

H. Witte is with the Institute of Medical Statistics, Computer Sciences and Documentation, Friedrich Schiller University, 07743 Jena, Germany (e-mail: herbert.witte@mti.uni-jena.de).

A. Colosimo and F. Babiloni are with the Human Physiology and Pharmacology Department, University of Rome "Sapienza," 00185 Rome, Italy (e-mail: colosimo@caspur.it; fabio.babiloni@uniroma1.it).

Color versions of one or more of the figures in this paper are available online at http://ieeexplore.ieee.org.

Digital Object Identifier 10.1109/TNSRE.2008.2006196

I. Introduction

OVER the last decade, there has been a growing interest in the detection of the functional connectivity in the brain from different neuroelectromagnetic and hemodynamic signals recorded by several neuroimaging devices such as the functional magnetic resonance imaging (fMRI) scanner, electroencephalography (EEG), and magnetoencephalography (MEG) apparatus [1]. Many methods have been proposed and discussed in the literature with the aim of estimating the functional relationships among different cerebral structures [2], [3]. However, the necessity of an objective comprehension of the network composed by the functional links of different brain regions is assuming an essential role in the neuroscience. Consequently, there is a wide interest in the development and validation of mathematical tools that are appropriate to spot significant features that could describe concisely the structure of the estimated cerebral networks [4]–[7]. The extraction of salient characteristics from brain connectivity patterns is an open challenging topic, since often the estimated cerebral networks have a relative large size and complex structure. Recently, it was realized that the functional connectivity networks estimated from actual brain-imaging technologies (MEG, fMRI, and EEG) can be analyzed by means of the graph theory (see [8] for a recent review). Since a graph is a mathematical representation of a network, which is essentially reduced to nodes and connections between them, the use of a theoretical graph approach seems relevant and useful as first demonstrated on a set of anatomical brain networks [9], [10]. In those studies, the authors have employed two characteristic measures, the average shortest path L and the clustering index C, to extract, respectively, the global and local properties of the network structure [11]. They have found that anatomical brain networks exhibit many local connections—i.e., a high C—and few random long distance connections—i.e., a low L. These values identify a particular model that interpolate between a regular lattice and a random structure. Such a model has been designated as "small-world" network in analogy with the concept of the small-world phenomenon observed more than 30 years ago in social systems [12]. In a similar way, many types of functional brain networks have been analyzed according to this mathematical approach. In particular, several studies based on different imaging techniques—fMRI [6], [13], [14], MEG [15]–[17], and EEG [18], [19]—have found that the estimated

1534-4320/$25.00 © 2008 IEEE

functional networks showed small-world characteristics. In the functional brain connectivity context, these properties have been demonstrated to reflect an optimal architecture for the information processing and propagation among the involved cerebral structures [20], [21]. However, the performance of cognitive and motor tasks as well as the presence of neural diseases has been demonstrated to affect such a small-world topology, as revealed by the significant changes of L and C. Moreover, some functional brain networks have been mostly found to be very unlike the random graphs in their degreedistribution [13], which gives information about the allocation of the functional links within the connectivity pattern. It was demonstrated that the degree distributions of these networks follow a power-law trend [22]. For this reason those networks are called "scale-free." They still exhibit the small-world phenomenon but tend to contain few nodes that act as highly connected "hubs." Scale-free networks are known to show resistance to failure, facility of synchronization and fast signal processing [20]. Hence, it would be important to see whether the scaling properties of the functional brain networks are altered under various pathologies or experimental tasks [23]. Besides these advanced indexes able to extract the global properties of the network structure, further measures are available from graph theory and some of them should be taken into account in order to inspect the other local basic properties belonging to the brain networks. In the present work, we propose a body of theoretical graph indexes in order to evaluate the functional network estimated from high-resolution EEG recordings in a group of healthy subjects during the performance of a simple motor task. In particular, we focused the attention to the preparation and to the execution of the foot movement by estimating the time-varying functional connectivity in the frequency domain. In this way, we were able to track the temporal evolution of the graph indexes computed from the obtained networks during the whole period of interest.

II. Methods

A. High-Resolution EEG

High-resolution EEG technology has been developed to enhance the poor spatial information of the EEG activity on the scalp and it gives a measure of the electrical activity on the cortical surface [24]–[26]. Principally, this technique involves the use of a larger number of scalp electrodes (64–256). In addition, high-resolution EEG uses realistic MRI-constructed subject head models [27], [28] and spatial de-convolution estimations which are commonly computed by solving a linear inverse problem based on boundary-element mathematics [29]. In the present study, the cortical activity was estimated from EEG recordings by using a realistic head model, whose cortical surface consisted of about 5000 triangles disposed uniformly. Each triangle represents the electrical dipole of a particular neuronal population and the estimation of its current density was computed by solving the linear inverse problem according to techniques described in previous works [30], [31]. In this way, the electrical activity in different regions of interest (ROIs) can be obtained by averaging the current density of the various dipoles within the considered cortical area.

B. Time-Varying Connectivity

The oscillatory behavior of the brain electrical activity indicates that frequency coding is one of the major candidates of its functioning [32]. Hence, many methods have been developed to estimate functional connections between brain areas in the frequency domain by using EEG or MEG recordings [2]. Among these, the partial directed coherence or partial directed coherence (PDC) [33] is a spectral measure used to determine the directed influences between any given pair of signals in a multivariate data set. It is computed from a multivariate auto-regressive model (MVAR) that simultaneously models the whole set of signals. In particular, this measure has been demonstrated to rely on the Granger causality concept (1969) [34], according to which an observed time series *x(n)* can be said to cause another series *y(n)* when the prediction error for *y(n)* at the present time is reduced by the knowledge of *x(n)*'s past measurements. As recently stressed in [35], the multivariate approach avoids the problem for the estimation of spurious functional links, which are very common with conventional bivariate approaches like, for instance, the ordinary coherence. In particular, the PDC is obtained from a unique MVAR model estimated on the entire set of trials according to the method proposed by Ding [36]. The MVAR estimators have been already applied to high-resolution EEG signals in order to achieve functional connectivity networks during motor tasks (in normal subjects and spinal cord injured patients) and also during cognitive tasks [30], [31], [37]–[39]. To overcome the limits of the classical definition of PDC, (mainly the request of stationarity of the data) a time-varying method for the estimation of PDC was recently introduced [40], [41]. In these studies, the time-varying connectivity was based on an adaptive approach. The time dependent parameter matrices were estimated by means of the recursive least squares (RLS) algorithm with forgetting factor, as described in [42], [59]. In particular, the RLS algorithm represents a particular variant of the Kalman Filter. This recursive estimator for the aMVAR-parameter is characterized by a more universal practicability since it requires less computational effort and it is possible to extend this approach to the presence of multiple realizations of the same process. The extension to multiple trials was introduced by Moller [42] and [59]. The fitting procedure of the AR parameters, exploits the RLS technique with the use of a forgetting factor. It is based on the minimization of the sum of exponentially weighted prediction errors of the process past. Thereby, the weighting depends on an adaptation constant $0 \leq c < 1$ which controls the compromise between adaptation speed and the quality of the estimation. Values close to zero result in a slower adaptation with more stable estimations and vice versa. Finally, a mean MVAR fits a set of trials, each one representing the measurement of the same task. A comprehensive description of the algorithms may be found in [42], [43], and [59].

C. Theoretical Graph Indexes

A graph is an abstract representation of a network. It consists of a set of vertexes—or nodes—and a set of edges—or connec-

tions—indicating the presence of some of interaction between the vertexes. The adjacency matrix A contains the information about the connectivity structure of the graph. When a weighted and directed edge exists from the node i to j, the corresponding entry of the adjacency matrix is $A_{ij} \neq 0$; otherwise $A_{ij} = 0$.

1) Network Density: The simplest attribute for a graph is its density *k*, defined as the actual number of connections within the model divided by its maximal capacity; density ranges from 0 to 1, the sparser is a graph, the lower is its value. When dealing with weighted networks, a useful generalization of this quantity is represented by the weighted-density k_w, which evaluates the intensities of the links composing the network. The mathematical formulation of the network density is given by the following:

$$k_w(A) = \sum_{i \neq j \in V} w_{ij} \tag{1}$$

where *A* is the adjacency matrix and w_{ij} is the weight of the respective arc from the point j to the point i. $V = 1 \ldots N$ is the set of nodes within the graph. The weighted-density gives information about the level of overall connectivity and constitutes the basis for correct analysis of all other graph parameters.

2) Node Strength: In the same way, the simplest attribute of a node is its connectivity degree, which is the total number of connections with other vertexes. In a weighted graph, the natural generalization of the degree of a node i is the node strength or node weight or weighted degree [40]. This quantity has to be split into in strength s_{in} and out strength s_{out}, when directed relationships are being considered. The strength index integrates the information of the links' number (degrees) with the connections' weight, thus representing the total amount of outgoing intensity from a node or incident intensity into it. The formulation of the in strength index s_{in} can be introduced as follows:

$$s_{\text{in}}(i) = \sum_{j \in V} w_{ij}. \tag{2}$$

It represents the whole functional flow incoming to the vertex i. V is the set of the available nodes and w_{ij} is the weight of the particular arc from the point j to the point i. In a similar way, for the out strength

$$s_{\text{out}}(i) = \sum_{j \in V} w_{ji}. \tag{3}$$

It represents the whole functional flow outgoing from the vertex *i*.

3) Strength Distribution: For a weighted graph, the arithmetical average of all the nodes' strengths $\langle s \rangle$ only gives little information about the distributions of the links intensity within the system. Hence, it is useful to introduce $R(s)$ as the fraction of vertexes in the graph that have strength equal to *s*. In the same way, $R(s)$ is the probability that a vertex chosen uniformly at random has weight $= s$. A plot of $R(s)$ for any network can be constructed by making a histogram of the vertexes' strength. This histogram represents the strength distribution of the graph and allows a better understanding of the strength allocation in the system. In particular, when dealing with directed graphs, the strength distribution has to be split in order to consider in a separated way the contribution of the incoming and outgoing flows.

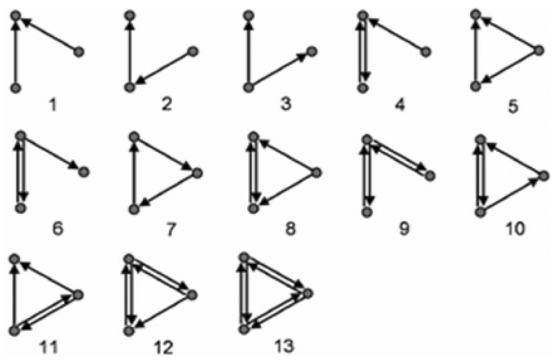

Fig. 1. Composition and numeration of all the possible directed motifs with three nodes (three-motifs).

4) Link Reciprocity: In a directed network, the analysis of link reciprocity reflects the tendency of vertex pairs to form mutual connections between each other [44]. Here, we computed the correlation coefficient index ρ proposed by Garlaschelli and Loffredo [45], which measures whether double links—with opposite directions—occur between vertex pairs more or less often than expected by chance. The correlation coefficient can be written as follows:

$$\rho(A) = \frac{r(A) - k_w(A)}{1 - k_w(A)}. \tag{4}$$

In this formula, *r* is the ratio between the number of links pointing in both directions and the total number of links, while k_w is the connection density that equals the average probability of finding a reciprocal link between two connected vertexes in a random network. As a measure of reciprocity, ρ is an absolute quantity that directly allows one to distinguish between reciprocal $(\rho > 0)$ and anti-reciprocal $(\rho < 0)$ networks, with mutual links occurring more and less often than random, respectively. The neutral or areciprocal case corresponds to $\rho = 0$. Note that if all links occur in reciprocal pairs one has $\rho = 1$, as expected.

5) Motifs: By motif it is usually meant a small connected graph of M vertexes and a set of edges forming a subgraph of a larger network with $N > M$ nodes. For each N, there are a limited number of distinct motifs. For $N = 3, 4$, and 5, the corresponding numbers of directed motifs is 13, 199, and 9364 [46]. In this work, we focus on directed motifs with $N = 3$. The 13 different three-node directed motifs are shown in Fig. 1. Counting how many times a motif appears in a given network yields a frequency spectrum that contains important information on the network basic building blocks. Eventually, one can looks at those motifs within the considered network that occur at a frequency significantly higher than in random graphs [44]. It must be noted that the application of the PDC techniques on the high-resolution EEG data returns a weighted and directed graph, showing the statistically significant connections between the analyzed ROIs. However, for the motif detection we used the methods already tested for several unweighted networks, as previously suggested in the literature [47], [58]. In addition, the unweighted motifs analysis has been recently used for the study of anatomical brain networks [48]. In order to apply such a method

we converted the statistically significant links within the functional brain networks into unweighted connections (if the edge weight was >0, then we changed it into 1).

6) Network Structure: Two measures are frequently used to characterize the local and global structure of unweighted graphs: the average shortest path L and the clustering index C [11], [49], [50]. The former measures the efficiency of the passage of information among the nodes, the latter indicates the tendency of the network to form highly connected clusters of vertexes. Recently, a more general setup has been examined in order to investigate weighted networks [51]. In particular, Latora and Marchiori [52] considered weighted networks and defined the efficiency coefficient e of the path between two vertexes as the inverse of the shortest distance between the vertexes (note that in weighted graphs the shortest path is not necessarily the path with the smallest number of edges). In the case where a path does not exist, the distance is infinite and $e = 0$. The average of all the pair-wise efficiencies e_{ij} is the global efficiency E_g of the graph. Thus, global efficiency can be defined as

$$E_g(A) = \frac{1}{N(N-1)} \sum_{i \neq j \in V} \frac{1}{d_{i,j}} \tag{5}$$

where N is the number of vertexes composing the graph. Since the efficiency e also applies to disconnected graphs, the local properties of the graph can be characterized by evaluating for every vertex i the efficiency coefficients of A_i, which is the subgraph composed by the neighbors of the node i. The local efficiency E_l is the average of all the subgraphs global efficiencies

$$E_l(A) = \frac{1}{N} \sum_{i \in V} E_{\text{glob}}(A_i). \tag{6}$$

Since the node i does not belong to the subgraph A_i, this measure reveals the level of fault-tolerance of the system, showing how the communication is efficient between the first neighbors of i, when i is removed. Global- (E_g) and local-efficiency (E_l) were demonstrated to reflect the same properties of the inverse of the average shortest path $1/L$ and the clustering index C [53]. Hence, the definition of small-world can be rephrased and generalized in terms of the efficiency indexes [8], [51]. Small-world networks have high E_g (i.e., high $1/L$) and high E_l (i.e., high C). This new definition is attractive since it takes into account the full information contained in the weighted links of the graph and provides an elegant solution to handle disconnected vertexes.

D. Application to Real Data

1) Experimental Design: Five voluntary and healthy subjects participated in the study (age, 26–32 years; five males). They had no personal history of neurological or psychiatric disorder, and they were free from medications, alcohol, or drugs abuse. For the EEG data acquisition, subjects were comfortably seated on a reclining chair in an electrically shielded and dimly lit room. They were asked to perform a dorsal flexion of their right foot. The motor task was repeated every 8 s in a self-paced manner and 200 single trials were recorded by using a 200-Hz sampling frequency. A 96-channel system (BrainAmp, Brainproducts GmbH, Germany) was used to record EEG and EMG electrical potentials by means of an electrode cap and surface electrodes, respectively. The electrode cap was built accordingly to an extension of the 10–20 international system to 64 channels. Structural MRIs of the subject's head were taken with a Siemens 1.5-T Vision Magnetom MR system (Germany). Three-dimensional electrode positions were obtained by using a photogrammetric localization (Photomodeler, Eos Systems Inc., Vancouver, BC, Canada) with respect to anatomic landmarks: nasion and the two preauricular points. Trained neurologists visually inspected EEG data and trials containing artifacts were rejected. Subsequently, they were baseline adjusted and low-pass filtered at 45 Hz. In order to inspect the brain dynamics during the preparation and the execution of the studied movement, a time segment of 2 s was analyzed, after having centered it on the onset detected by a tibial EMG. The most interesting cerebral processes concerning the detected movement are actually thought to occur within this interval [54].

2) Cortical Connectivity: In agreement with the procedure already described previously in the literature [30], [31], the 5000 time series estimated for each cortical dipole were collapsed (by spatial averaging) in 16 time varying waveforms related to the activity of each considered ROIs. The sixteen ROIs were segmented from the cortical model of each subject. The ROIs considered for the left (_L) and right (_R) hemisphere were the primary motor areas of the foot (MF_L and MF_R), the proper supplementary motor areas (SM_L and SM_R), and the cingulate motor areas (CM_L and CM_R). The bilateral Brodmann areas 6 (6_L and 6_R), 7 (7_L and 7_R), 8 (8_L and 8_R), 9 (9_L and 9_R), and 40 (40_L and 40_R) were also considered. In the following, these cortical regions represent the nodes of the modeling graph. This data reduction allowed dealing with mathematically treatable MVAR processes for the estimation of the significant PDC links. Moreover, due to the fact that in the present experiment only 16 ROIs were considered the correction for the multiple comparisons was performed by taking into account only $(16^2 - 16)$ comparisons. The PDC was then normalized, and the normalization was performed on the activity entering in each node. The model order was chosen by means of the Akaike information criterion (AIC), applied to different representative intervals using the mean prediction error. Based on the recommendations suggested by Schack [55] we finally chose the maximal order detected. The order of the used aMVAR models ranged from 14 to 16 for all the experimental subjects. The application of the PDC to the 16 cortical waveforms returned a weighted and directed network for each frequency band of interest. In the present work, we analyzed the Alpha (7–12 Hz) band.

3) Significant Links: The rough connectivity estimation produces a full connected weighted and asymmetric matrix, representing the Granger-causal influences among all the cortical regions of interest. In order to consider only the task-related connections, a filtering procedure based on a statistical validation was adopted. In each trial, a rest period of 2 s preceding the movement was selected as element of contrast (from -4 to -2 s before the onset). The connection intensities regarding the pairs of ROIs for each time sample were collected in order to obtain,

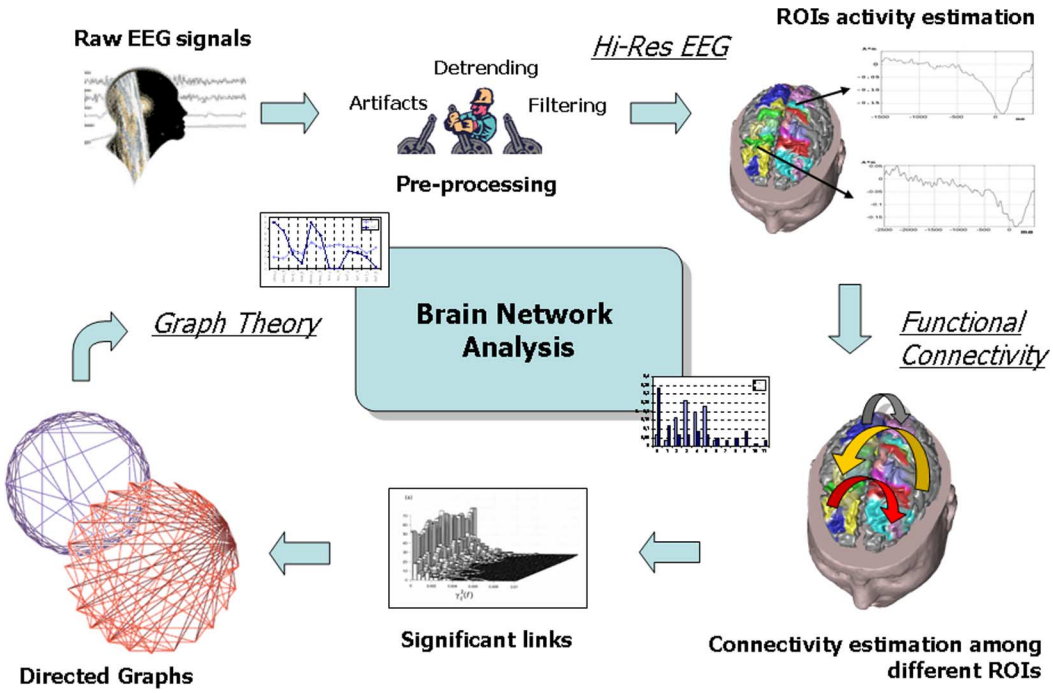

Fig. 2. Schematic representation of the main steps involved in the EEG data processing. From raw EEG signals, the cortical activity is achieved by means of high-resolution EEG techniques. Then, functional connectivity is estimated from the cortical time series and eventually the brain network analysis is performed through a theoretical graph approach.

a distribution of values belonging to the rest period. A threshold range was then extracted from the values of the rest distribution by considering a percentile of 0.01 and 0.99, respectively, for the lowest and highest edge, with the aim of testing the significance of the estimated connections throughout the period of interest. After the statistical filtering, the remaining connections represent the significant relationships among the ROIs that characterize the experimental task.

4) Statistical Comparison With Random Graphs: A contrast with random graphs was performed in order to assess the significance of the obtained graph indexes. For each frequency band and time-sample, 50 random patterns were generated from the cerebral network of each subject, by randomly shuffling the original connections. In the present study, the randomization procedure does not preserve the degree distributions. This choice was suggested by the fact that the networks we are dealing with are rather small. For this reason, the degree distribution preservation could not lead to evident differences in the structure contrast. A common number of connections has been considered in each graph in order to analyze the cortical networks correctly across all the subjects, frequency bands, and time samples. This condition prevents that the graph measures could be affected by a different connection-density. In the present study, we considered 48 edges—i.e., connection density $= 0.2$—for each network obtained by removing the weakest links from each weighted graph. The preference of this connection-density was surely the most favorable condition for the significance of the indexes of the network structure (E_g and E_l). At a more specific analysis, it has been found that these indexes keep their usual independency—characterized by their ability to detect global and local properties—even in a small 16 nodes-graph (data not shown here). Fig. 2 summarizes the main methodological steps of the EEG data processing that was performed in the present work.

III. Results

In the following, we show the results obtained from the use of theoretical graph methodology applied to the EEG signals recorded in a group of healthy subjects performing a simple motor act. As described above, the use of the time-varying PDC on the high-resolution EEG signals returns a cortical network for each time sample and for each frequency band. In the present work, we intend to focus the analysis on a representative spectral range—namely the Alpha band—since it has been suggested as particular responsive to the preparation and execution of a simple limb movement [54]. The whole time progress of the strength indexes during the analyzed period of interest-2 s—was computed for each cortical region of interest ROI. At the middle of Fig. 3, the locations of the ROIs are illustrated in color on the realistic model of the cortex. At the lateral sides of Fig. 3, the average Z-scores of the in strength indexes s_{in} obtained in the Alpha band are illustrated for the ROIs strictly related to the movement. It is worth of note that during the large part of the movement preparation and execution, the in strength values of the cingulate (CM_L, CM_R) and supplementary (SM_L, SM_R) motor areas are significantly $(p < 0.05)$ high throughout the analyzed period. Instead, the primary motor areas (MF_L, MF_R) only present few significant moments $(Z > 1.96)$. At the top of Fig. 3 the average Z values of the time-varying in strength distribution R_{in} in the Alpha frequency band, are illustrated. The color encodes the intensity of the computed Z value for the R_{in} index. This measure reveals the significant presence of ROIs that have an in strength value s_{in} (y axes) at the time t (x axes). In general

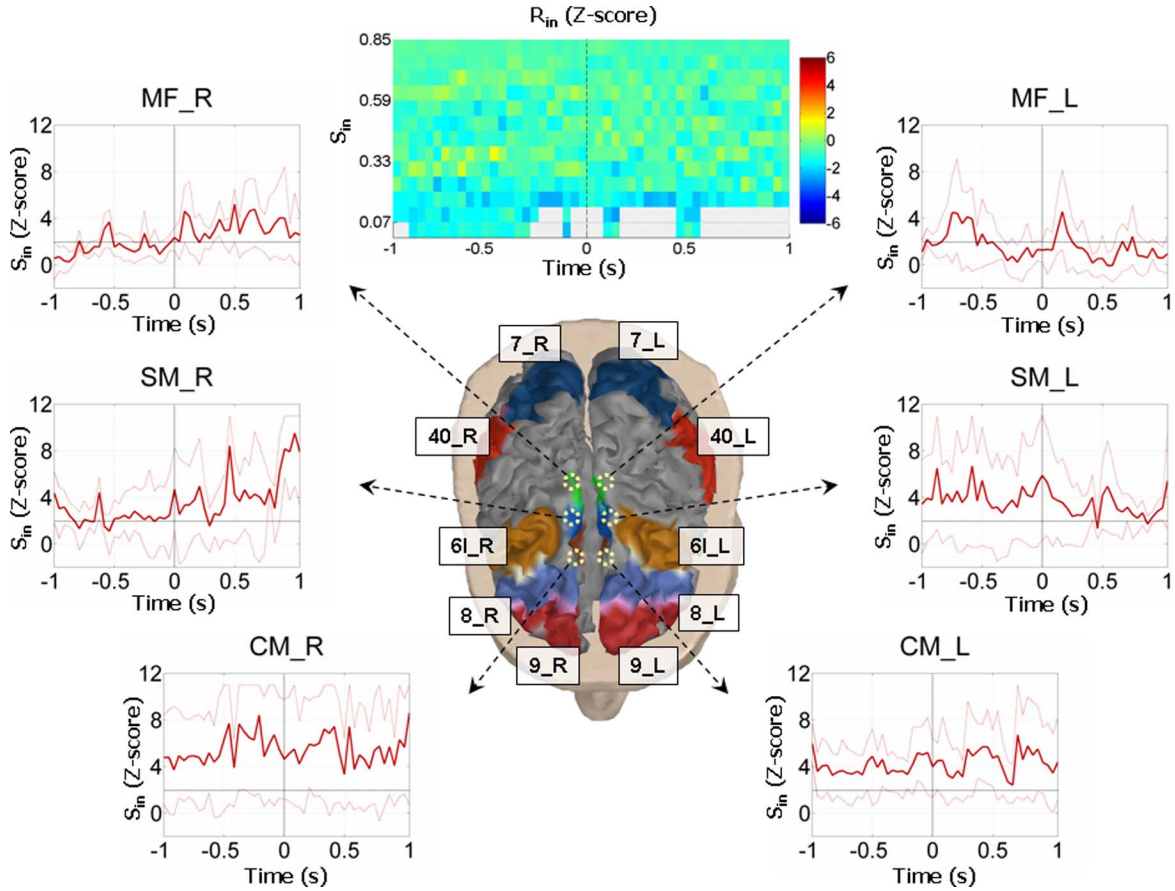

Fig. 3. *Middle*: Realistic head model for a representative subject. All the cortical ROIs are displayed in color on the cortex and opportunely labeled. *Lateral*: Representation of the time-varying in strength index $s_{\rm in}$ in the Alpha band. Each subplot describes the group-averaged *Z* score of a particular cortical region during the entire period of the task. The latency from the movement onset is shown on the *x* axes. The lighter lines around the mean value indicate the profiles of the 25th and 75th percentile. *Top*: Representation of the time-varying in strength distribution $R_{\rm in}$ during the period of interest in the Alpha band. The latency from the movement onset is shown on the *x* axes; the in strength $(s_{\rm in})$ values on the *y* axes. The color encodes the group-averaged intensity of the $R_{\rm in}$ *Z* score. In particular, the light grey color stands for the absence of ROIs with $s_{\rm in} > 0$ at a certain instants.

it is evident that the overall *Z* scores of $R_{\rm in}$ are not statistically significant, with many values between -1.96 and 1.96. With the same conventions as in the previous picture, Fig. 4 shows the results obtained for the out strength measures. As regards the out strengths indexes $s_{\rm out}$, only the CM_L and CM_R present a persistent and significant high level of involvement. Moreover, the out strength distribution $R_{\rm out}$ index reveals that the intensity of outgoing links seems to increase as time elapses from the movement preparation to the movement execution. This fact can be noted by the shift of the significant *Z* values towards high levels of $s_{\rm out}$ throughout the evolution of the task performance. Fig. 5(A) shows the functional connectivity patterns in the Alpha frequency band during three representative moments. In particular, each network shows the intensity of the connections for a particular experimental subject. One arrow from the node *X* to the node *Y* indicates the existence of a statistically significant Granger-causality relationship between the cortical areas they are representing. Fig. 5(B) shows the average time-varying course of the weighted-density k_w in the Alpha band during the analyzed period of interest. A progressive increase during the preparation of the movement can be observed. Instead, during the execution of the movement the cortical network holds steady high k_w values. Fig. 5 (C) and (D) shows, respectively, the average Z scores of the time-varying E_g and E_l computed from the connectivity patterns in the Alpha frequency band. The analysis of the network structure indexes shows a general stable time-course of low E_g and high E_l during the preparation and the execution of the foot movement. However, the time varying profile of these indexes revealed the presence of several peaks that characterize some temporal points. In particular, the efficiency indexes clearly assumed an opposite behavior at about 500 ms after the movement onset, with very low E_g $(Z < -6)$ and high E_l $(Z > 4)$, indicating a wide presence of highly connected clusters that improved the local interactions of the cortical network. The reciprocity indexes were gathered from the cortical network of all the subjects in each time instant. In Fig. 6(A) the average time-varying trend of the correlation coefficient ρ is shown for the representative Alpha frequency band. In particular, from the movement preparation to the movement execution the reciprocity measure of the cortical networks moves from a relative high reciprocal state $(\rho \sim 0.25)$ to a lower $(\rho \sim 0.1)$ level, as revealed by the decreasing trend of the index profile. The involvement of the basic building blocks within the estimated time-varying functional networks was analyzed by means of the motifs spectra. Fig. 6(B) shows the average *Z* values of the time

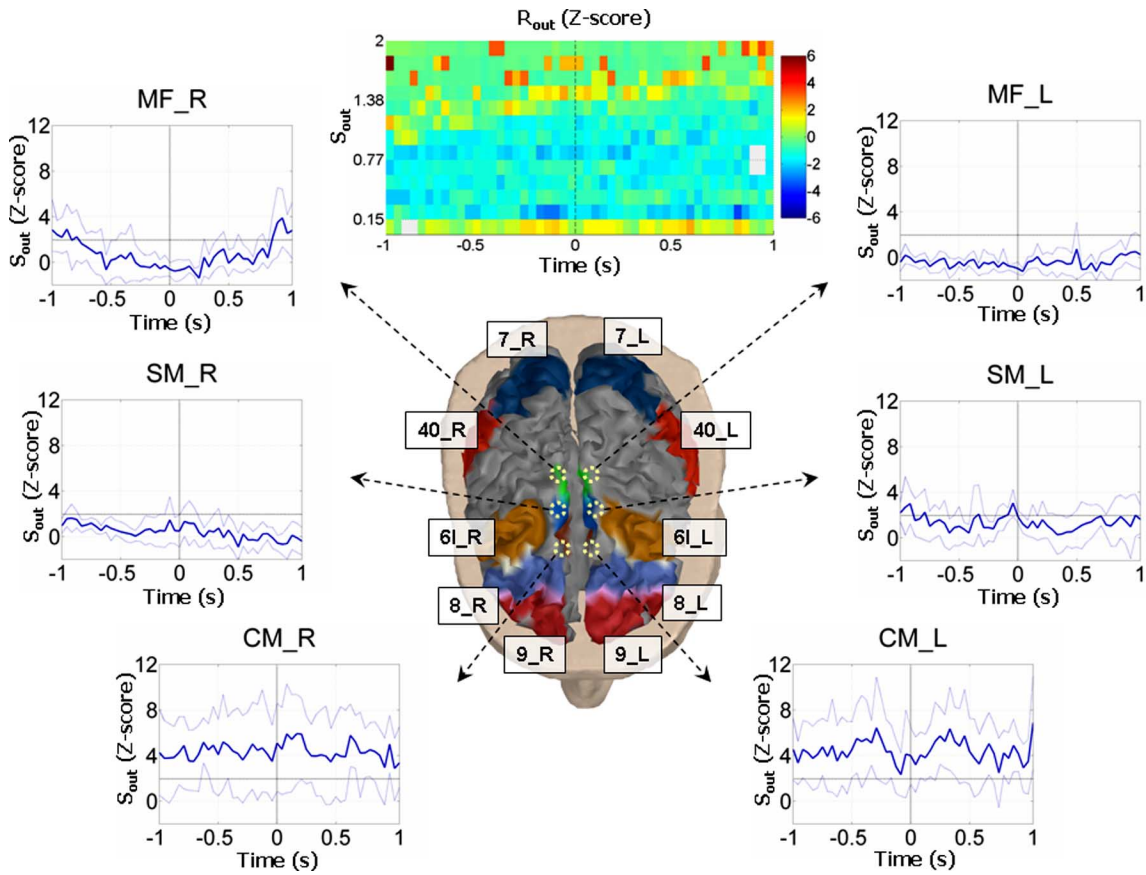

Fig. 4. Representation of the time-varying out strength index s_{out} and out strength distribution R_{out} in the Alpha band. Same conventions as in Fig. 3.

varying motifs spectrum in the Alpha band. On the ordinates all the possible 13 motif classes with three nodes are listed. On the abscissas, the time in seconds is displayed while the grey scale codes the average values of the resulting *Z*-scores. The significant $(p < 0.01)$ role of two type of building blocks (the third and the eleventh called, respectively, "single-input" and "uplinked-mutual-dyad") is revealed by the persistent high *Z* values $(Z \gg 1.96)$ observed during the entire period of interest. In addition, the fifth motif (called "feed-forward-loop") presents an interesting involvement. Its general profile shows that it moves from a nonsignificant presence during the movement preparation (from about -1 to the onset) to a significant $(p < 0.05)$ presence during the movement execution (from the onset to $+1$ s), as revealed by the higher *Z* values $(Z > 1.96)$.

IV. Discussion

The use of graph theory in small networks is rather new if compared to its usual employment in biological context. However, the need for the analysis of small cerebral networks has been recently underlined [18], [19], [56]. In the present study, we would like to emphasize that the opportunity to deal with cortical activity permits the representation of the graph nodes as particular Brodmann areas on the cortex [57]. The use of raw EEG signals instead returns less powerful results, since the nodes within the network represent scalp electrodes, which could have indirect links with the cortical areas beneath them. In this context, the adaptive PDC could represent a major improvement in the analysis and interpretation of EEG and MEG data. In fact, the possibility to deal explicitly with weighted and asymmetric relationships, as well as the observation of transient couplings, would provide the analytical tools to observe the specific cortical network dynamics during the task. Since the present work would represent a methodological study, we presented results in a particular spectral content (i.e., Alpha 7–12 Hz), which represents one of the most responsive channels for the preparation and the execution of simple motor acts [54]. As a demonstration of the effectiveness of the methodology here presented, some indexes deriving from graph theory have been applied to the time-varying networks estimated from a set of high-resolution EEG data in a group of healthy subjects during the preparation and the execution of the foot movement. The analysis of the strength indexes in the Alpha band revealed the major involvement of particular cortical areas throughout the task. The high *Z* values of in and out strength for the cingulate motor areas (CM_L, CM_R) indicate that they presented the main target for a large number of functional connections taking origin from the other investigated cortical areas and, at the same time, they represented the main sources of outgoing flows towards all the other ROIs. It is worth of note that the PDC was normalized, and the normalization was performed on the activity entering in each node. It may be argued if such normalization has an effect on the statistical assessment of in strength s_{in} and out strength s_{out} values. However, s_{in} and s_{out} were computed on statistically significant values of PDC, which were assessed by

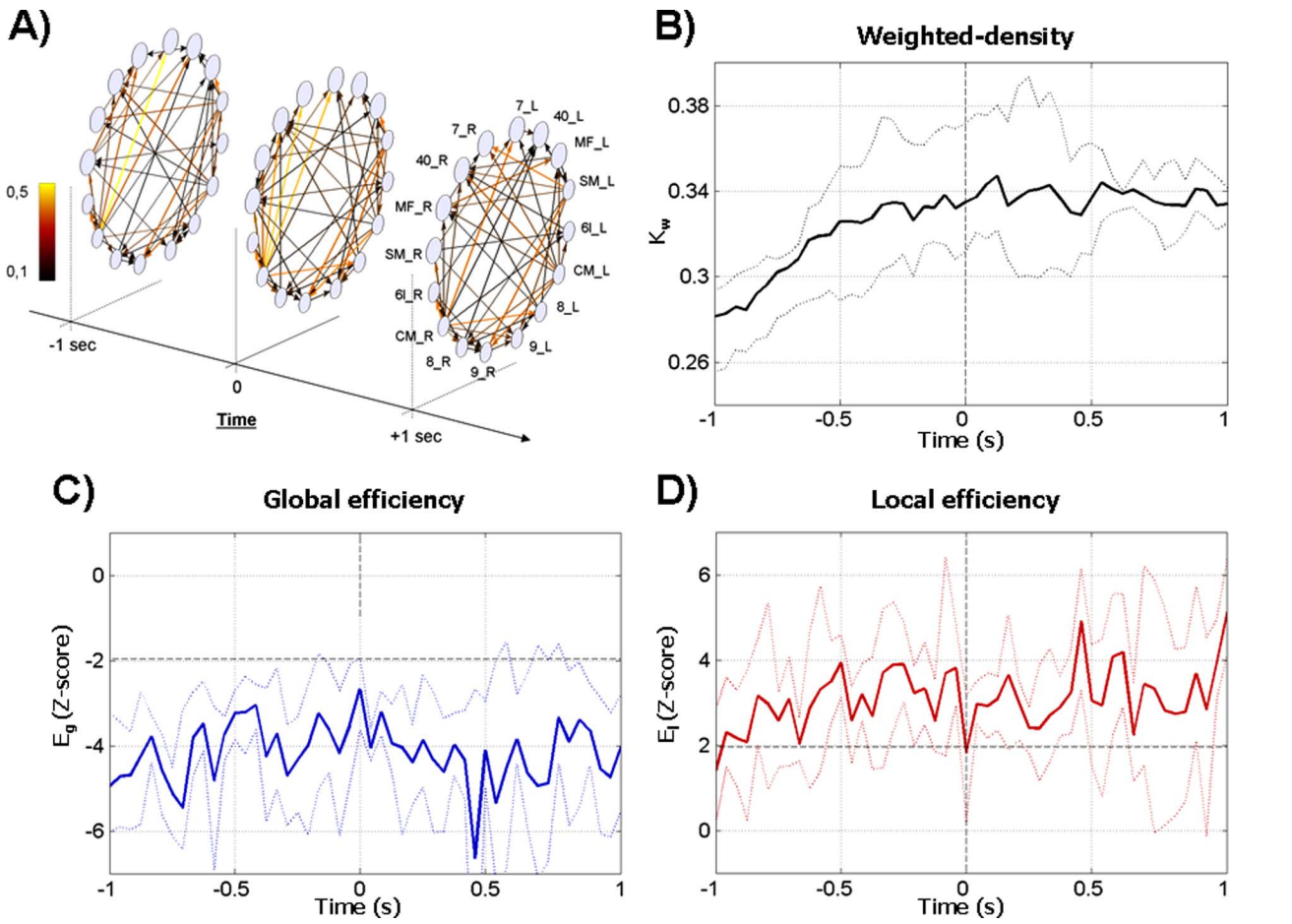

Fig. 5. (A) Representation of the functional networks—as graphs—in the Alpha frequency band at three particular time-points. Granger-causality from an area *X* to *Y* is represented by an arrow; the intensity of this relationship is coded by its size and color. The lighter and bigger is the arrow, the higher is the intensity. (B) Group-averaged time-varying weighted-density k_w during the whole time period in the Alpha band. The lighter lines around the mean value indicate the time courses of the 25th and 75th percentile. The latency from the movement onset is shown on the *x* axes. (C) Group-averaged time-varying global-efficiency E_g in the Alpha band. The blue line represents the evolving average *Z* score. The lighter lines around the mean value indicate the time courses of the 25th and 75th percentile. The latency from the movement onset is shown on the *x* axes. (D) Group-averaged time-varying global-efficiency E_l in the Alpha band. The red line represents the evolving average *Z* score. Same conventions as in Fig. 5(C).

taking into account the normalization performed. Later, we evaluated the *Z* score of such indexes with respect to the same indexes obtained from random networks. Since separate analyses were performed to the two different parameters, the normalization has not an affect on such assessment. The average profiles of the strength-distributions revealed a different behavior between the distributions of the incoming and outgoing strength indexes. In fact, the out strength distribution only indicated a significant $(p < 0.01)$ presence of few cortical areas acting as "hubs," characterized by a very high level of outgoing functional flows. Looking more closely at the strength values of the ROIs previously analyzed, we can deduce that the CM_L and CM_R operated as the center of outgoing flows for the estimated cortical functional network. This fact suggests a central role of the cingulate motor areas, which hold the highest level of outgoing links, since their removal would immediately corrupt the organization of the estimated functional network by reducing the overall level of connectivity. Interestingly, it may be observed that the out strength *Z* scores of the contralateral cortex MF_L is almost nonsignificant $(Z < 2)$ throughout the entire period of analysis. A similar behavior can be also observed for other cortical sites that are related to the movement (SM_L, SM_R, and MF_R). However, this lack of significant outgoing connections from the contralateral primary motor cortex does not mean or imply a low activity of such cortex. In fact, the analyzed index (s_{out}) only measures the amount of actual statistically significant connections outgoing from the considered cortical area (in such a case the primary motor area of the foot) to the other ones. A zero value of this parameter means that the considered cortical area still remains active in a "disconnected" way, i.e., without having particular connections with other cortical areas. This is consistent with the view that the primary cortical areas are prone to deliver the motor commands for the actual execution of the movement, while the other cortical areas have to perform the coordination about the necessary timing of the operation. In particular, it must be emphasized that each flow is actually representing a "Granger" causal interaction between two active cortical areas. For this reason, a significant out strength value should not be interpreted as a significant "activity" of a specific ROI. In fact, graph indexes and electrical activity belong to different levels of analysis and the respective results/conclusions may put in evidence on different ROIs of the analyzed

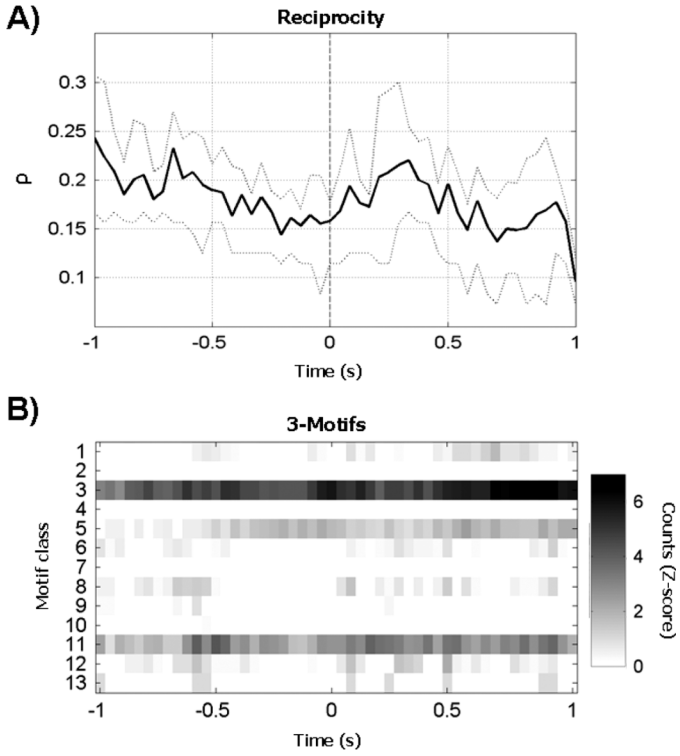

Fig. 6. (A) Group-averaged time-varying reciprocity-index ρ during the period of interest in the Alpha band. On y axes the correlation coefficient ρ, while time in seconds is displayed on x axes. Dotted lines represent the 25th and 75th percentiles. (B) Representation for the group-average of the time-varying three-motifs spectra in the Alpha band. On y axes all the 13 possible directed three-motifs are listed, while time in seconds is displayed on x axes. The grey-scale encodes the group-average of the obtained Z values after the contrast with random graphs.

cortex. As a matter of fact, in the acquired EEG data we were able to observe the typical strong event-related desynchronization [54] in proximity of the movement onset for the contralateral cortex MF_L. This activity is typically very high for the motor areas when they are engaged in motor tasks. The evaluation of the average weighted-density k_w associated to the evolution of the cortical network returned further information regarding the varying level of overall connectivity. In the Alpha band, the average intensity of the network links showed a characteristic increase during the preparation (from -0.5 s to the onset) of the movement, reflecting the need for a higher exchange of information among the considered ROIs in order to perform the subsequent movement execution. The study of the structural properties of the cortical network was performed by calculating the global-efficiency E_g and the local-efficiency E_l. In the Alpha band, the network structure seemed to maintain a steady configuration, since the efficiency indexes remained in the significant $(p < 0.05)$ part, with low E_g and high E_l throughout the analyzed period. In particular, these values identified a regular and ordered configuration [11], in which the local property of clustering is privileged with respect to the overall communication. Besides this consideration, the evolving nature of the calculated indexes allowed for the extraction of characteristic time points. In particular, the presence of clustering connections reached its maximum rate during the proper execution of the movement at about 500 ms after the onset. The analysis of the average time-varying reciprocity index revealed the significant presence of mutual links within the cortical networks during the entire period analyzed. In particular, in the Alpha frequency band the functional network moved from a high $(\rho \sim 0.25)$ to a lower $(\rho \sim 0.1)$ reciprocal state following a decreasing trend throughout the movement. This aspect emphasizes the role of the preparation in which a higher level of mutual exchange of information is required to speed up the cortical process in expectation of the subsequent execution. In the present study, we dealt with rather small cortical networks of sixteen nodes, derived by the analysis of the time-varying waveforms estimated from each considered ROI. For this reason, the research of the three-motifs seems a reasonable approach. Larger motifs could be justified within larger cortical networks than those employed here. In particular, the average time-varying spectra of the three-motifs revealed the involvement of the feed-forward-loop motif that tends to significantly $(p < 0.01)$ increase during the proper movement execution (from about 0 to $+1$ s). This type of building block is known to play an important functional role in information processing. In fact, one possible function of this circuit is to activate output only if the input signal is persistent and to allow a rapid deactivation when the input goes off [58]. Another interesting aspect was revealed by the significant $(p < 0.01)$ "persistence" of the single-input motif that represented the highest recurrent pattern of interconnections within the cortical network during the entire evolution of the foot movement. The main function of this motif is known to involve the "activation" of several parallel pathways by a single activator [58]. Altogether, our findings aim at proving how the use of some theoretical graph measures were able to extract important information about the time-frequency dynamics of the cortical networks estimated from a set of high-resolution EEG data during the performance of a simple foot movement. In particular, the obtained results are rather stable across subjects as revealed by the small dispersion of the estimated graph values. This fact reflects a small variability in the structure of the estimated connectivity patterns. The present paper intends to support the development of a mathematical tool consisting in a body of indexes based on the graph theory. In this way, the "brain network analysis" (in analogy with the social network analysis that has emerged as a key technique in modern sociology) could actually represent an effective methodology to improve the comprehension of the complex interactions in the brain.

REFERENCES

[1] B. Horwitz, "The elusive concept of brain connectivity," *NeuroImage*, vol. 19, pp. 466–470, 2003.
[2] O. David, D. Cosmelli, and K. J. Friston, "Evaluation of different measures of functional connectivity using a neural mass model," *NeuroImage*, vol. 21, no. 2, pp. 659–673, 2004.
[3] L. Lee, L. M. Harrison, and A. Mechelli, "The functional brain connectivity workshop: Report and commentary," *NeuroImage*, vol. 19, pp. 457–465, 2003.
[4] G. Tononi, O. Sporns, and G. M. Edelman, "A measure for brain complexity: Relating functional segregation and integration in the nervous system," in *Proc. Nat. Acad. Sci. USA*, 1994, vol. 91, pp. 5033–5037.
[5] C. J. Stam, "Functional connectivity patterns of human magnetoencephalographic recordings: A "small-world" network?," *Neurosci. Lett.*, vol. 355, pp. 25–28, 2004.

[6] R. Salvador, J. Suckling, M. R. Coleman, J. D. Pickard, D. Menon, and E. Bullmore, "Neurophysiological architecture of functional magnetic resonance images of human brain," *Cereb. Cortex*, vol. 15, no. 9, pp. 1332–1342, 2005.

[7] O. Sporns, , R. Kötter, Ed., "Graph theory methods for the analysis of neural connectivity patterns," in *Neuroscience Databases. A Practical Guide*. Norwell, MA: Kluwer, 2002, pp. 171–186.

[8] C. J. Stam and J. C. Reijneveld, "Graph theoretical analysis of complex networks in the brain," *Nonlinear Biomed. Phys.*, vol. 1, 2007.

[9] S. H. Strogatz, "Exploring complex networks," *Nature*, vol. 410, pp. 268–276, 2001.

[10] O. Sporns, , R. Kötter, Ed., "2002 Graph theory methods for the analysis of neural connectivity patterns," in *Neuroscience Databases. A Practical Guide*. Norwell, MA: Kluwer, pp. 171–186.

[11] D. J. Watts and S. H. Strogatz, "Collective dynamics of "small-world" networks," *Nature*, vol. 393, pp. 440–442, 1998.

[12] S. Milgram, "The small world problem," *Psychol. Today*, pp. 60–67, 1967.

[13] V. M. Eguiluz, D. R. Chialvo, G. A. Cecchi, M. Baliki, and A. V. Apkarian, "Scale-free brain functional networks," *Phys. Rev. Lett.*, vol. 94, p. 018102, 2005.

[14] S. Achard and E. Bullmore, "Efficiency and cost of economical brain functional networks," *PLoS Comp. Biol.*, vol. 3, no. 2, p. e17, 2007.

[15] C. J. Stam, B. F. Jones, I. Manshanden, A. M. van Cappellen van Walsum, T. Montez, J. P. Verbunt, J. C. de Munck, B. W. van Dijk, H. W. Berendse, and P. Scheltens, "Magnetoencephalographic evaluation of resting-state functional connectivity in Alzheimer's disease," *NeuroImage*, vol. 32, pp. 1335–1344, 2006.

[16] D. S. Bassett, A. Meyer-Linderberg, S. Achard, Th. Duke, and E. Bullmore, "Adaptive reconfiguration of fractal small-world human brain functional networks," *Proc. Nat. Acad. Sci.*, vol. 103, pp. 19518–19523, 2006.

[17] F. Bartolomei, I. Bosma, M. Klein, J. C. Baayen, J. C. Reijneveld, T. J. Postma, J. J. Heimans, B. W. van Dijk, J. C. de Munck, A. de Jongh, K. S. Cover, and C. J. Stam, "Disturbed functional connectivity in brain tumour patients: Evaluation by graph analysis of synchronization matrices," *Clin. Neurophysiol.*, vol. 117, pp. 2039–2049, 2006.

[18] S. Micheloyannis, E. Pachou, C. J. Stam, M. Vourkas, S. Erimaki, and V. Tsirka, "Using graph theoretical analysis of multi channel EEG to evaluate the neural efficiency hypothesis," *Neurosci. Lett.*, vol. 402, pp. 273–277, 2006.

[19] C. J. Stam, B. F. Jones, G. Nolte, M. Breakspear, and Ph. Scheltens, "Small-world networks and functional connectivity in Alzheimer's disease," *Cereb. Cortex*, vol. 17, pp. 92–99, 2007.

[20] L. F. Lago-Fernandez, R. Huerta, F. Corbacho, and J. A. Siguenza, "Fast response and temporal coherent oscillations in small-world networks," *Phys. Rev. Lett.*, vol. 84, pp. 2758–2761, 2000.

[21] O. Sporns, G. Tononi, and G. E. Edelman, "Connectivity and complexity: The relationship between neuroanatomy and brain dynamics," *Neural Netw.*, vol. 13, pp. 909–922, 2000.

[22] A. L. Barabasi and R. Albert, "Emergence of scaling in random networks," *Science*, vol. 286, pp. 509–512, 1999.

[23] S. Achard, R. Salvador, B. Whitcher, J. Suckling, and Bullmore, Eds., "A resilient low-frequency, small-world human brain functional network with highly connected association cortical hubs," *J. Neurosci.*, vol. 26, no. 1, pp. 63–72, 2006.

[24] J. Le and A. Gevins, "A method to reduce blur distortion from EEG's using a realistic head model," *IEEE Trans. Biomed. Eng.*, vol. 40, no. 6, pp. 517–528, Jun. 1993.

[25] A. Gevins, J. Le, N. Martin, P. Brickett, J. Desmond, and B. Reutter, "High resolution EEG: 124-channel recording, spatial deblurring and MRI integration methods," *Electroenceph. Clin. Neurophysiol.*, vol. 39, pp. 337–358, 1994.

[26] P. L. Nunez, *Neocortical Dynamics and Human EEG Rhythms*. New York: Oxford Univ. Press, 1995, p. 708.

[27] F. Babiloni, C. Babiloni, F. Carducci, L. Fattorini, C. Anello, P. Onorati, and A. Urbano, "High resolution EEG: A new model-dependent spatial deblurring method using a realistically-shaped MR-constructed subject's head model," *Electroenceph. Clin. Neurophysiol.*, vol. 102, pp. 69–80, 1997.

[28] F. Babiloni, C. Babiloni, L. Locche, F. Cincotti, P. M. Rossini, and F. Carducci, "High resolution EEG: Source estimates of Laplacian-transformed somatosensory-evoked potentials using a realistic subject head model constructed from magnetic resonance images," *Med. Biol. Eng. Comput.*, vol. 38, pp. 512–519, 2000.

[29] M. R. Grave de Peralta and A. S. L. Gonzalez, , C. Uhl, Ed., "Distributed source models: Standard solutions and new developments," in *Analysis of Neurophysiological Brain Functioning*. New York: Springer Verlag, 1999, pp. 176–201.

[30] F. Babiloni, F. Cincotti, C. Babiloni, F. Carducci, A. Basilisco, P. M. Rossini, D. Mattia, L. Astolfi, L. Ding, Y. Ni, K. Cheng, K. Christine, J. Sweeney, and B. He, "Estimation of the cortical functional connectivity with the multimodal integration of high resolution EEG and fMRI data by directed transfer function," *NeuroImage*, vol. 24, no. 1, pp. 118–123, 2005.

[31] L. Astolfi, F. Cincotti, C. Babiloni, F. Carducci, A. Basilisco, P. M. Rossini, S. Salinari, D. Mattia, S. Cerutti, D. Ben Dayan, L. Ding, Y. Ni, B. He, and F. Babiloni, "Estimation of the cortical connectivity by high resolution EEG and structural equation modeling: Simulations and application to finger tapping data," *IEEE Trans. Biomed. Eng.*, vol. 52, no. 5, pp. 757–768, May 2005.

[32] E. Basar, *Memory and Brain Dynamics: Oscillations Integrating Attention, Perception, Learning and Memory*. Boca Raton, FL: CRC, 2004.

[33] K. Sameshima and L. A. Baccala, "Using partial directed coherence to describe neuronal ensemble interactions," *J. Neurosci. Methods*, vol. 94, pp. 93–103, 1999.

[34] C. W. J. Granger, "Investigating causal relations by econometric models and cross-spectral methods," *Econometrica.*, vol. 37, pp. 424–438, 1969.

[35] R. Kus, M. Kaminski, and K. J. Blinowska, "Determination of EEG activity propagation: Pair-wise versus multichannel estimate," *IEEE Trans. Biomed. Eng.*, vol. 51, no. 9, pp. 1501–1510, Sep. 2004.

[36] M. Ding, S. L. Bressler, W. Yang, and H. Liang, "Short-window spectral analysis of cortical event-related potentials by adaptive multivariate autoregressive modeling: Data preprocessing, model validation, and variability assessment," *Biol. Cybern.*, vol. 83, pp. 35–45, 2000.

[37] L. Astolfi, F. Cincotti, D. Mattia, M. G. Marciani, L. Baccalà, F. De Vico Fallani, S. Salinari, M. Ursino, M. Zavaglia, L. Ding, J. C. Edgar, G. A. Miller, B. He, and F. Babiloni, "A comparison of different cortical connectivity estimators for high resolution EEG recordings," *Human Brain Mapp.*, vol. 28, no. 2, pp. 143–157, 2006.

[38] L. Astolfi, F. De Vico Fallani, F. Cincotti, D. Mattia, M. G. Marciani, S. Bufalari, S. Salinari, A. Colosimo, L. Ding, J. C. Edgar, W. Heller, G. A. Miller, B. He, and F. Babiloni, "Imaging functional brain connectivity patterns from high-resolution EEG and fMRI via graph theory," *Psychophysiology*, vol. 44, no. 6, pp. 880–893, 2007.

[39] F. De Vico Fallani, L. Astolfi, F. Cincotti, D. Mattia, M. G. Marciani, S. Salinari, J. Kurths, S. Gao, A. Cichocki, A. Colosimo, and F. Babiloni, "Cortical functional connectivity networks in normal and spinal cord injured patients: Evaluation by graph analysis," *Hum. Brain Mapp.*, vol. 28, pp. 1334–1336, 2007.

[40] L. Astolfi, F. Cincotti, D. Mattia, F. De Vico Fallani, A. Tocci, A. Colosimo, S. Salinari, M. G. Marciani, W. Hesse, H. Witte, M. Ursino, M. Zavaglia, and F. Babiloni, "Tracking the time-varying cortical connectivity patterns by adaptive multivariate estimators," *IEEE Trans. Biomed. Eng.*, vol. 55, no. 3, pp. 902–913, Mar. 2008.

[41] M. Winterhalder, B. Schelter, W. Hesse, K. Schwabb, L. Leistritz, D. Klan, R. Bauer, J. Timmer, and H. Witte, "Comparison of linear signal processing techniques toinfer directed interactions in multivariate neural systems," *Signal Process.*, vol. 85, no. 11, pp. 2137–2160, 2005.

[42] E. Moeller, B. Schack, M. Arnold, and H. Witte, "Instantaneous multivariate EEG coherence analysis by means of adaptive high-dimensional autoregressive models," *J. Neurosci. Methods*, vol. 105, p. 143/58, 2001.

[43] W. Hesse, E. Möller, M. Arnold, and B. Schack, "The use of time-variant EEG Granger causality for inspecting directed interdependencies of neural assemblies," *J. Neurosci. Methods*, vol. 124, pp. 27–44, 2003.

[44] S. Wasserman and K. Faust, *Social Network Analysis*. Cambridge, U.K.: Cambridge Univ. Press, 1994.

[45] D. Garlaschelli and M. I. Loffredo, "Patterns of link reciprocity in directed networks," *Phys. Rev. Lett.*, vol. 93, p. 268701, 2004.

[46] F. Harary and E. M. Palmer, *Graphical Enumeration*. New York: Academic, 1973, p. 124.

[47] R. Milo, S. Shen-Orr, S. Itzkovitz, N. Kashtan, D. Chklovskii, and U. Alon, "Network motifs: Simple building blocks of complex networks," *Science*, vol. 298, pp. 824–827, 2002.

[48] O. Sporns and R. Kötter, "Motifs in brain networks," *PLoS Biol.*, vol. 2, p. e369, 2004.

[49] M. E. J. Newman, "The structure and function of complex networks," *SIAM Rev.*, vol. 45, pp. 167–256, 2003.

[50] M. G. Grigorov, "Global properties of biological networks," *Drug Discovery Today*, vol. 10, pp. 365–372, 2005.
[51] S. Boccaletti, V. Latora, Y. Moreno, M. Chavez, and D. U. Hwang, "Complex networks: Structure and dynamics," *Phys. Rep.*, vol. 424, pp. 175–308, 2006.
[52] V. Latora and M. Marchiori, "Efficient behaviour of small-world networks," *Phys. Rev. Lett.*, vol. 87, p. 198701, 2001.
[53] V. Latora and M. Marchiori, "Economic small-world behaviour in weighted networks," *Eur. Phys. JB*, vol. 32, pp. 249–263, 2003.
[54] G. Pfurtsheller and F. H. Lopes da Silva, "Event-related EEG/EMG synchronizations and desynchronization: Basic principles," *Clin. Neurophysiol.*, vol. 110, pp. 1842–1857, 1999.
[55] B. Schack, "Dynamic topographic spectral analysis of cognitive processes," in *Analysis of Neurophysiological Brain Functioning*. New York: Springer, 1999, pp. 230–251.
[56] C. C. Hilgetag, G. A. P. C. Burns, M. A. O'Neill, J. W. Scannell, and M. P. Young, "Anatomical connectivity defines the organization of clusters of cortical areas in the macaque monkey and the cat," *Philos. Trans. R. Soc. Lond. B. Biol. Sci.*, vol. 355, pp. 91–110, 2000.
[57] F. De Vico Fallani, L. Astolfi, F. Cincotti, D. Mattia, A. Tocci, M. G. Marciani, A. Colosimo, S. Salinari, S. Gao, A. Cichocki, and F. Babiloni, "Extracting information from cortical connectivity patterns estimated from high resolution EEG recordings: A theoretical graph approach," *Brain Topogr.*, vol. 19, no. 3, pp. 125–136, 2007.
[58] S. Shen-Orr, R. Milo, S. Mangan, and U. Alon, "Network motifs in the transcriptional regulation network of Escherichia Coli," *Nature Genetics*, vol. 31, pp. 64–68, 2002.
[59] S. H. Yook, H. Jeong, A. Barabási, and Y. Tu, "Weighted evolving networks," *Phys. Rev. Lett.*, vol. 86, no. 25, pp. 5835–5838, 2001, [40].

Authors' photographs and biographies not available at the time of publication.